RESEARCH ARTICLE

WILEY

Relationship between topological efficiency of white matter structural connectome and plasma biomarkers across the Alzheimer's disease continuum

Mingkai Zhang[1] | Haojie Chen[2,3,4] | Weijie Huang[2,3,4] | Tengfei Guo[5] | Guolin Ma[6] | Ying Han[1,5,7,8,9] | Ni Shu[2,3,4]

[1]Department of Neurology, Xuanwu Hospital, Capital Medical University, Beijing, China

[2]State Key Laboratory of Cognitive Neuroscience and Learning & IDG/McGovern Institute for Brain Research, Beijing Normal University, Beijing, China

[3]BABRI Centre, Beijing Normal University, Beijing, China

[4]Beijing Key Laboratory of Brain Imaging and Connectomics, Beijing Normal University, Beijing, China

[5]Institute of Biomedical Engineering, Shenzhen Bay Laboratory, Shenzhen, China

[6]Department of Radiology, China-Japan Friendship Hospital, Beijing, China

[7]School of Biomedical Engineering, Hainan University, Haikou, China

[8]National Clinical Research Center for Geriatric Diseases, Beijing, China

[9]Center of Alzheimer's Disease, Beijing Institute for Brain Disorders, Beijing, China

Correspondence
Ying Han, School of Biomedical Engineering, Hainan University, Haikou 570228, China.
Email: hanying@xwh.ccmu.edu.cn

Ni Shu, No. 19, Xinjiekouwai St, Haidian District, Beijing 100875, China.
Email: nshu@bnu.edu.cn

Abstract

Both plasma biomarkers and brain network topology have shown great potential in the early diagnosis of Alzheimer's disease (AD). However, the specific associations between plasma AD biomarkers, structural network topology, and cognition across the AD continuum have yet to be fully elucidated. This retrospective study evaluated participants from the Sino Longitudinal Study of Cognitive Decline cohort between September 2009 and October 2022 with available blood samples or 3.0-T MRI brain scans. Plasma biomarker levels were measured using the Single Molecule Array platform, including β-amyloid (Aβ), phosphorylated tau181 (p-tau181), glial fibrillary acidic protein (GFAP), and neurofilament light chain (NfL). The topological structure of brain white matter was assessed using network efficiency. Trend analyses were carried out to evaluate the alterations of the plasma markers and network efficiency with AD progression. Correlation and mediation analyses were conducted to further explore the relationships among plasma markers, network efficiency, and cognitive performance across the AD continuum. Among the plasma markers, GFAP emerged as the most sensitive marker (linear trend: $t = 11.164$, $p = 3.59 \times 10^{-24}$; quadratic trend: $t = 7.708$, $p = 2.25 \times 10^{-13}$; adjusted $R^2 = 0.475$), followed by NfL (linear trend: $t = 6.542$, $p = 2.9 \times 10^{-10}$; quadratic trend: $t = 3.896$, $p = 1.22 \times 10^{-4}$; adjusted

Mingkai Zhang and Haojie Chen contributed equally to this study.

$R^2 = 0.330$), p-tau181 (linear trend: $t = 8.452$, $p = 1.61 \times 10^{-15}$; quadratic trend: $t = 6.316$, $p = 1.05 \times 10^{-9}$; adjusted $R^2 = 0.346$) and Aβ42/Aβ40 (linear trend: $t = -3.257$, $p = 1.27 \times 10^{-3}$; quadratic trend: $t = -1.662$, $p = 9.76 \times 10^{-2}$; adjusted $R^2 = 0.101$). Local efficiency decreased in brain regions across the frontal and temporal cortex and striatum. The principal component of local efficiency within these regions was correlated with GFAP (Pearson's $R = -0.61$, $p = 6.3 \times 10^{-7}$), NfL ($R = -0.57$, $p = 6.4 \times 10^{-6}$), and p-tau181 ($R = -0.48$, $p = 2.0 \times 10^{-4}$). Moreover, network efficiency mediated the relationship between general cognition and GFAP (ab = -0.224, 95% confidence interval [CI] = [-0.417 to -0.029], $p = .0196$ for MMSE; ab = -0.198, 95% CI = [-0.42 to -0.003], $p = .0438$ for MOCA) or NfL (ab = -0.224, 95% CI = [-0.417 to -0.029], $p = .0196$ for MMSE; ab = -0.198, 95% CI = [-0.42 to -0.003], $p = .0438$ for MOCA). Our findings suggest that network efficiency mediates the association between plasma biomarkers, specifically GFAP and NfL, and cognitive performance in the context of AD progression, thus highlighting the potential utility of network-plasma approaches for early detection, monitoring, and intervention strategies in the management of AD.

KEYWORDS

Alzheimer's disease, Biomarker, Efficiency, Glial fibrillary acidic protein, Graph theory, Network, Neurofilament light chain, Plasma

1 | INTRODUCTION

Alzheimer's disease (AD) is a progressive neurodegenerative disorder characterized by cognitive decline, memory loss, and the inability to perform daily activities (Ballard et al., 2011). As the most common form of dementia, AD accounts for an estimated 60%–80% of dementia cases worldwide, and the number of individuals with AD is expected to nearly triple by 2050 (Anon, 2021; Hebert et al., 2013). The current lack of a cure and the irreversible nature of AD highlight the critical importance of early diagnosis, particularly at the preclinical stage. While biomarker detection in cerebrospinal fluid (CSF) and positron emission tomography (PET) imaging has advanced preclinical diagnosis (Jack et al., 2018), there remains a pressing need to explore practical, noninvasive, and cost-effective methods for identifying preclinical AD features.

A growing body of evidence implies that the pathophysiologic process of AD begins 15–20 years before the onset of clinical symptoms, especially in biomarkers and neuroimaging (Jack et al., 2018; Wang et al., 2020). With the rapid development of ultrasensitive assays, it is now possible to measure trace levels of brain-specific proteins in the blood (Andreasson et al., 2016). Plasma biomarkers are playing an increasingly important role in this area. Recent studies have shown that amyloid-β (Aβ) 42/40 and phosphorylated tau (p-tau) from plasma appear to be the best candidate markers during both symptomatic AD and preclinical AD (Nakamura et al., 2018; Ovod et al., 2017). While blood levels of neurofilament light (NfL) and glial fibrillary acidic protein (GFAP) are abnormal in a range of neurodegenerative disorders, there is a growing body of research that explores the potential of these markers as biomarkers for AD (Benedet et al., 2021; Mattsson et al., 2019). A recent investigation revealed that plasma levels of GFAP experience a noteworthy elevation during the preclinical stage of AD (Guo et al., 2023). Moreover, plasma GFAP exhibits the most effective performance for monitoring longitudinal disease progression (Chatterjee et al., 2022). Despite the potential of plasma biomarkers as diagnostic tools in routine clinical practice, their diagnostic efficacy alone may still fall short of being sufficient.

With the development of brain imaging and network modeling techniques, human brain connectomics has provided valuable insights into understanding dynamic neuronal network changes at the system level in various brain disorders (Bassett & Sporns, 2017). As a disconnection syndrome, AD is characterized by both structural and functional network changes throughout its continuum (Chen et al., 2023; Yu et al., 2021). With diffusion MRI, our previous studies have demonstrated decreased topological efficiency of the white matter (WM) structural network in amnestic mild cognitive impairment (MCI) and subjective cognitive decline (SCD) patients (Shu et al., 2018), especially involving key regions of the default mode network and striatum network (Rasero et al., 2017). Structural network efficiency measures the brain's infrastructure supporting interneuronal communication (Bassett & Sporns, 2017). Recent investigations have unveiled a significant correlation between network efficiency, AD pathology, and relevant biomarkers (Yu et al., 2021). Specifically, a noticeable decline in local efficiency with AD progression has been detected (Prescott et al., 2014), with these changes closely associated with hallmark pathological features, including Aβ deposition and tau tangles (Jonkman et al., 2020; Kocagoncu et al., 2020).

The interplay between pathological molecules in plasma and cognitive decline during the progression of AD constitutes a complex and multifaceted topic. One possible mechanism by which GFAP influences cognitive function is through glial activation and neuroinflammation (Bellaver et al., 2023). Simultaneously, plasma levels of NfL may impact cognitive function in AD through various pathways, including brain atrophy, neuronal damage, and glucose hypometabolism (Mattsson et al., 2019). Notably, we emphasize the mediating role of brain imaging-based biomarkers in the relationship between cognitive function and plasma biomarkers in AD (Moscoso et al., 2021). However, there is a paucity of comprehensive studies investigating the relationship between plasma biomarkers, neuronal networks, and cognition. Thus, the objectives of the present study are threefold: (1) to explore the dynamic changes in plasma biomarkers related to AD, specifically GFAP, across different stages of the AD continuum; (2) to investigate the dynamic alterations in brain network efficiency within AD-related regions; and (3) to assess the associations between brain network efficiency, plasma markers, and cognitive performance across the AD continuum.

2 | METHODS

2.1 | Participants

In this study, all participants were enrolled in the Sino Longitudinal Study of Cognitive Decline (SILCODE) cohort. SILCODE is an ongoing prospective multicentre AD cohort study in the Han population of mainland China (Li et al., 2019). A total of 474 participants were recruited, and all participants were divided into different data sets depending on research needs: plasma data set (complete data on AD-related plasma markers were available for each participant), imaging data set (each participant had complete imaging data available for brain network analysis), and combined data set (participants in the first two data sets who matched plasma and imaging time differences for no more than 80 days). A flow chart of participant selection is available in Figure S1.

The diagnosis of normal controls (NCs) was based on the exclusion of MCI and dementia (Albert et al., 2011; Bondi et al., 2014), requiring a CDR score of 0, no overt affective disorder, and normal MMSE scores for the education subdomain (greater than 17 for illiterate individuals, 20 for those with primary school education, and 24 for participants with middle school or higher education) and memory subdomain. Diagnostic criteria for SCD rely on defining and characterizing SCD (Jessen et al., 2020). The diagnosis of MCI was made based on neuropsychological criteria (Bondi et al., 2014). To qualify for AD dementia, the entry criteria must meet the proposed criteria for probable AD-induced dementia (Albert et al., 2011). Ultimately, the plasma data set ($n = 287$) included 121 NC, 107 SCD, 41 MCI, and 18 AD. The imaging data set ($n = 395$) included 129 NCs, 112 SCD patients, 17 MCI patients, and 7 AD patients. The combined data set ($n = 55$) included 25 NCs, 17 SCD patients, 8 MCI patients, and 5 AD patients.

All participants or their legal guardians provided written informed consent. All procedures were approved by the Medical Research Ethics Committee and Institutional Review Board of Xuanwu Hospital. The cohorts were registered with ClinicalTrials.gov (SILCODE: NCT03370744). For each participant, clinical data were collected, including age, gender, years of education, and apolipoprotein E (APOE) genotype. Neuropsychological assessments were administered to evaluate global cognitive function, including the Mini-Mental State Examination (MMSE) and Montreal Cognitive Assessment-Basic Version (MoCA-B) (Chen et al., 2016).

2.2 | Plasma biomarkers

Blood samples (2 mL venous blood) were taken between 7:00 and 8:00 in the morning after an overnight fast using EDTA tubes, and blood samples were collected in the following manner. Supernatants were collected as plasma after being centrifuged several times for 15 min at 4°C (speed: 2500 g/min). All plasma samples were stored at −80°C and immediately thawed on ice before assay. Plasma levels of β-amyloid (Aβ), phosphorylated tau181 (p-tau181), GFAP, and NFL were measured using the Single Molecule Array (Simoa™) platform (Quanterix Corporation, Billerica, MA, USA) following the manufacturer's instructions. The Simoa assays were performed using the following commercially available kits: β-amyloid (1–42) (Aβ42) and β-amyloid (1–40) (Aβ40)—Simoa™ β-Amyloid 42 (1–42) and β-Amyloid 40 (1–40) Advantage Kits, phosphorylated tau at threonine 181 (ptau181) Simoa™ p-tau181 Advantage Kit, GFAP Simoa™ GFAP Discovery Kit and Neurofilament light chain (NfL)—Simoa™ NF-light® Advantage Kit. All assays were performed in duplicate, and the average concentration values were reported. Sample concentrations below the lower limit of quantification (LLOQ) were assigned a value of half the LLOQ.

2.3 | Image acquisition and preprocessing

In the SILCODE cohort, MRI data were acquired using an integrated simultaneous 3.0 T TOF PET/MR (Siemens PET/MR, GE Healthcare, Milwaukee, WI, USA) at the Xuanwu Hospital of Capital Medical University, Beijing, China. Regarding SMRI, the parameters for T1-weighted 3D brain structural images were as follows: SPGR sequence, FOV = 256×256 mm^2, matrix = 256×256, slice thickness = 1 mm, gap = 0, slice number = 192, repetition time (TR) = 6.9 ms, echo time (TE) = 2.98 ms, inversion time (TI) = 450 ms, flip angle = 12°, and voxel size = $1 \times 1 \times 1$ mm^3. The DTI data were obtained with a single-shot spin–echo diffusion-weighted echo planar imaging sequence with the following parameters: FOV = 224×224 mm^2, data matrix = 112×112, slice thickness = 2 mm, gap = 0, slice number = 70, slice order = interleaved, TR = 16,500 ms, TE = 95.6 ms, 30 gradient directions ($b = 1000$ s/mm^2) and 5 b0 images, and voxel size = $2 \times 2 \times 2$ mm^3.

The preprocessing of diffusion MRI data involved denoising, head motion correction, and eddy current correction. Specifically, we first denoised the raw diffusion data with the **dwidenoise** command from MRtrix3 software (https://mrtrix.readthedocs.io/) (Tournier et al., 2019), which produced a denoised diffusion-weighted data file. The **fslroi** command was then used to extract a single volume from the denoised data, which was used as the reference image for head motion correction and brain extraction. The **bet2** command was applied to this reference image to obtain the brain mask. Finally, eddy current correction was performed using the **eddy_openmp** command with the denoised data, brain mask, and gradient information as inputs.

2.4 | Brain structural network construction

To construct the individual structural network, we used the **bet** command to extract the brain and the **fast** command to segment it into different tissue types on the T1-weighted image with FSL software (https://fsl.fmrib.ox.ac.uk/) (Jenkinson et al., 2012). The WM segmentation in T1 space was transformed into diffusion space and used as a seed mask for further tractography. The **Bedpostx** command was then performed on the preprocessed diffusion MRI data to generate distributions on diffusion parameters at each voxel, with three fibers modeled per voxel, burn-in period set to 3000, and deconvolution model with sticks. Deterministic tractography was performed using a **track** command from CAMINO software (http://camino.cs.ucl.ac.uk/) (Cook et al., 2005) with the "bedpostx_dyad" input model and various parameters, including nearest-neighbor interpolation, fourth-order Runge–Kutta method as the tracking algorithm, and tracking step size set to 2 mm. Compartments with a mean volume fraction below 0.1 were discarded, tracking was terminated if the curvature exceeded 45° degrees at each 5-mm interval, and fibers with a length below 20 mm or above 250 mm were removed. To define network nodes, the BNA template was applied and transformed into individual diffusion space to parcellate the brain into 246 regions (https://atlas.brainnetome.org/) (Fan et al., 2016). Finally, tractography and brain parcellation were combined to generate a streamline-number weighted connectivity matrix with the **conmat** command, representing the individual WM structural network.

2.5 | Network efficiency computation

Based on the brain structural network, we calculated three network efficiency measures with the BCT toolbox (https://www.nitrc.org/projects/bct/) (Rubinov & Sporns, 2010), including global efficiency, local efficiency, and generalized local efficiency. Each measure was calculated at both the regional and network levels. Here are the detailed descriptions of network efficiency measures:

Global efficiency reflects the integration of region i, which was calculated as

$$E_{glob}(i,N) = \frac{1}{n-1} \sum_{j \in N, j \neq i} \frac{1}{L_{i,j}},$$

where $L_{i,j}$ is the shortest path length between node i and node j within network N.

Local efficiency captures region i's segregation and fault tolerance capabilities, which was computed as the mean of global efficiency across all nodes encompassed within i's neighborhood:

$$E_{loc}(i,N) = \frac{1}{|N_i|} \sum_{j \in N_i} E_{glob}(j,N_i),$$

where N_i is the subnetwork of node i comprising i's neighbors with the connections among them (Figure 3b).

Generalized local efficiency enhances robustness against irrelevant factors and establishes weight-scale invariance (Wang et al., 2017), as calculated with

$$E_{loc}^Z(i,N) = \frac{1}{\max(W)^{\frac{1}{3}}} \frac{\sum_{j,h} w_{ij}^{1/3} w_{ih}^{1/3} \left[d_{jh}^w(N_i') \right]^{-1}}{\sum_{j,h} w_{ij}^{1/3} w_{ih}^{1/3}},$$

where $w_{i,j}$ is the weight (fiber-number) between region i and j, and $d_{jh}^w(N_i')$ is the adapted shortest distance between region j and h, calculated as the shortest distance in network N_i' containing all neighbors of i excluding node i while considering a replacement of the weight of the edge (j, h) to $w'_{jh} = w_{jh}^{1/3}$.

3 | STATISTICAL ANALYSIS

The demographic variables were analyzed using ANOVA for continuous variables, including age, years of education, MMSE scores, MOCA scores, levels of plasma markers, and network efficiency. For discrete variables such as sex, chi-squared tests were employed. These statistical analyses were performed across four diagnostic groups (NC, SCD, MCI, and AD) separately on three data sets: plasma, imaging, and combined data sets.

Trend ANCOVA (analyses of covariance) was then conducted to assess plasma markers, regional and whole-brain network efficiency, and cognitive performance, accounting for age, sex, years of education, and APOE4 status as covariates. Post hoc comparisons were performed on measures displaying significant linear or quadratic trends using two-sample t tests, with Bonferroni corrections applied. Separate analyses were conducted for plasma markers and network efficiency within the plasma and imaging data sets.

Correlation analyses were carried out to assess the relationships between plasma markers, network efficiency, and cognitive performance across the AD continuum. Partial correlations were evaluated between plasma markers and cognitive performances (MMSE and MOCA score) in the plasma data set and between network efficiency,

plasma markers, and cognitive performances in the combined data set. Linear models were used to control for the effects of age, sex, years of education, and APOE4 status before computing Pearson's R.

Additionally, the mediation of network efficiency in the relationship between plasma markers and cognition was examined using the mediation package. The significance of indirect effects and 95% confidence intervals (CIs) were obtained using bootstrapping procedures with 10,000 resamples. The effects of age, sex, years of education, and APOE4 status were accounted for by including them as covariates in the main effects and mediating effects paths. To enhance the reliability of the findings, we conducted a comprehensive robustness analysis, considering various bootstrap resample numbers ranging from 500 to 20,000 (Figure S4).

All statistical analyses were performed using R (version 4.1.1). For regional statistics, false discovery rate (FDR) corrections were applied in trend analyses and regional correlations. We considered significance at a nominal 5% level for corrected p values. Mediation effects were considered significant if the 95% CIs of the indirect effect did not include zero.

4 | RESULTS

4.1 | Cohort characteristics

Demographics of the plasma data set ($n = 287$), the imaging data set ($n = 395$), and the combined data set ($n = 55$) are separately presented in Table 1, Table S1, and Table 2. Among individuals with MCI and AD, we observed a higher likelihood of advanced age in the plasma data set ($p = .025$) and the combined data set ($p = .071$).

Additionally, MCI and AD patients exhibited significantly decreased cognitive performance ($p < .0001$) in the plasma data set. When considering plasma biomarkers, significant between-group differences were found for plasma NfL ($p < .001$), GFAP ($p < .0001$), and p-tau181 ($p < .0001$) in both the plasma and combined data sets. However, the plasma Aβ42/Aβ40 ratio was significant only in the plasma data set ($p < .001$), while no significant differences were observed for Aβ42 and Aβ40 ($p > .05$). Furthermore, whole-brain generalized local efficiency demonstrated significant differences in both the imaging data set and the combined data set ($p < .01$).

4.2 | Plasma markers related to AD progression

Across four diagnostic groups (NC, SCD, MCI, and AD), significant varying trends with AD progression for all four plasma markers were observed in the plasma data set. Specifically, GFAP emerged as the most sensitive marker (linear trend: $t = 11.164$, $p = 3.59 \times 10^{-24}$; quadratic trend: $t = 7.708$, $p = 2.25 \times 10^{-13}$; adjusted $R^2 = 0.475$), followed by NfL (linear trend: $t = 6.542$, $p = 2.9 \times 10^{-10}$; quadratic trend: $t = 3.896$, $p = 1.22 \times 10^{-4}$; adjusted $R^2 = 0.330$), p-tau181 (linear trend: $t = 8.452$, $p = 1.61 \times 10^{-15}$; quadratic trend: $t = 6.316$, $p = 1.05 \times 10^{-9}$; adjusted $R^2 = 0.346$), and Aβ42/Aβ40 (linear trend: $t = -3.257$, $p = 1.27 \times 10^{-3}$; quadratic trend: $t = -1.662$, $p = 9.76 \times 10^{-2}$; adjusted $R^2 = 0.101$) (Figure 1 and Table S2). We also observed significant correlations between these plasma markers and general cognitive performance in the plasma data set (Figure 2, $p < .00001$ for GFAP, NfL, and p-tau181. See Figure S2 for the correlation of all plasma markers and cognition).

TABLE 1 Sample characteristics in the blood data set.

	NC ($n = 121$)	SCD ($n = 107$)	MCI ($n = 41$)	AD ($n = 18$)	Overall ($n = 287$)	Statistics (p)
Sex (M/F)	42/79	33/74	19/22	7/11	101/186	3.243 (.518)
Age	69.0 ± 5.58	68.1 ± 7.28	69.8 ± 8.02	73.8 ± 6.81	69.1 ± 6.80	2.803 (.025)
Education	12.4 ± 3.17	13.2 ± 3.51	10.9 ± 4.05	12.4 ± 2.66	12.5 ± 3.48	3.418 (<.01)
APOEε4 carriers (percentage)	18.2%	34.6%	41.5%	66.7%	30.7%	22.862 (<.001)
MMSE	28.8 ± 1.19	28.6 ± 1.52	26.5 ± 2.63	15.4 ± 6.55	27.5 ± 3.93	73.054 (<.0001)
MoCA-B	25.7 ± 2.89	25.6 ± 2.48	21.6 ± 3.21	9.89 ± 5.94	24.1 ± 4.98	64.563 (<.0001)
Plasma Aβ42 (pg/mL)	6.26 ± 1.45	6.14 ± 1.53	6.22 ± 1.52	5.17 ± 1.60	6.14 ± 1.51	2.111 (.078)
Plasma Aβ40 (pg/mL)	104 ± 21.1	99.5 ± 21.6	108 ± 17.8	109 ± 26.9	103 ± 21.4	1.755 (.137)
Plasma Aβ42/Aβ40	0.0624 ± 0.0167	0.0623 ± 0.0106	0.0575 ± 0.0109	0.0482 ± 0.0095	0.0607 ± 0.0139	5.092 (<.001)
Plasma NfL (pg/mL)	16.2 ± 7.80	15.3 ± 6.66	20.0 ± 13.0	31.5 ± 14.0	17.4 ± 9.64	13.073 (<.0001)
Plasma GFAP (pg/mL)	126 ± 56.5	116 ± 54.0	156 ± 82.3	303 ± 88.9	138 ± 76.4	29.455 (<.0001)
Plasma p-tau181 (pg/mL)	2.03 ± 1.07	2.09 ± 0.91	2.35 ± 1.16	4.67 ± 1.50	2.27 ± 1.23	21.764 (<.0001)

Note: Continuous data are presented as the mean ± SD. Analyses of variance were utilized for continuous variables, while chi-square tests were employed for categorical variables across NC, SCD, MCI, and AD.

Abbreviations: Aβ, amyloid β; AD, Alzheimer's disease; APOE, apolipoprotein E; GFAP, glial fibrillary acidic protein; MCI, mild cognitive impairment; MMSE, Mini-Mental State Examination; MoCA-B, Montreal Cognitive Assessment Basic; NC, normal control; NfL, neurofilament light chain; p-tau, phosphorylated tau; SCD, subjective cognitive decline.

TABLE 2 Sample characteristics in the combined data set with network efficiency.

	NC ($n = 25$)	SCD ($n = 17$)	MCI ($n = 8$)	AD ($n = 5$)	Overall ($n = 55$)	Statistics (p)
Sex (M/F)	8/17	5/12	3/5	1/4	17/38	0.473 (.976)
Age	65.7 ± 4.98	61.4 ± 8.03	69.5 ± 9.55	69.2 ± 8.91	65.2 ± 7.53	2.228 (.071)
Education	12.6 ± 3.21	13.5 ± 3.94	13.1 ± 3.52	13.0 ± 4.24	13.0 ± 3.50	0.162 (.957)
APOEε4 carriers (percentage)	28.0%	35.3%	75.0%	40.0%	38.2%	5.76 (.218)
MMSE	28.8 ± 1.48	29.0 ± 1.17	24.8 ± 3.11	12.0 ± 7.91	26.7 ± 5.61	16.406 (<.0001)
MoCA-B	24.9 ± 3.88	26.5 ± 2.45	19.4 ± 2.83	8.80 ± 5.76	23.1 ± 6.17	13.688 (<.0001)
Plasma Aβ42 (pg/mL)	6.09 ± 1.21	5.71 ± 1.85	5.98 ± 1.27	4.84 ± 1.48	5.84 ± 1.47	0.808 (.523)
Plasma Aβ40 (pg/mL)	100 ± 20.2	93.5 ± 28.3	111 ± 15.5	96.9 ± 37.3	99.4 ± 24.2	0.754 (.558)
Plasma Aβ42/Aβ40	0.0631 ± 0.0155	0.0625 ± 0.0115	0.0540 ± 0.0102	0.0517 ± 0.00658	0.0605 ± 0.0135	1.358 (.253)
Plasma NfL (pg/mL)	15.1 ± 6.05	13.1 ± 4.82	18.8 ± 8.88	30.8 ± 7.68	16.4 ± 7.89	6.429 (<.001)
Plasma GFAP (pg/mL)	114 ± 47.6	113 ± 49.9	201 ± 105	359 ± 69.9	149 ± 94.7	11.43 (<.0001)
Plasma p-tau181 (pg/mL)	1.53 ± 0.526	1.88 ± 0.729	3.07 ± 1.32	4.66 ± 2.28	2.14 ± 1.34	8.887 (<.0001)
Global efficiency	6.55 ± 5.71	5.18 ± 2.94	5.05 ± 3.49	5.87 ± 6.30	5.85 ± 4.69	0.278 (.891)
Local efficiency	13.2 ± 13.4	10.5 ± 6.23	10.5 ± 7.73	12.3 ± 11.1	11.9 ± 10.5	0.21 (.932)
Generalized local efficiency	0.242 ± 0.0175	0.249 ± 0.0112	0.245 ± 0.0211	0.213 ± 0.0167	0.242 ± 0.0186	4.182 (<.01)

Note: Continuous data are presented as the mean ± SD. Analyses of variance were utilized for continuous variables, while chi-square tests were employed for categorical variables across NC, SCD, MCI, and AD.

Abbreviations: Aβ, amyloid β; AD, Alzheimer's disease; APOE, apolipoprotein E; GFAP, glial fibrillary acidic protein; MCI, mild cognitive impairment; MMSE, Mini-Mental State Examination; MoCA-B, Montreal Cognitive Assessment Basic; NC, normal control; NfL, neurofilament light chain; p-tau, phosphorylated tau; SCD, subjective cognitive decline.
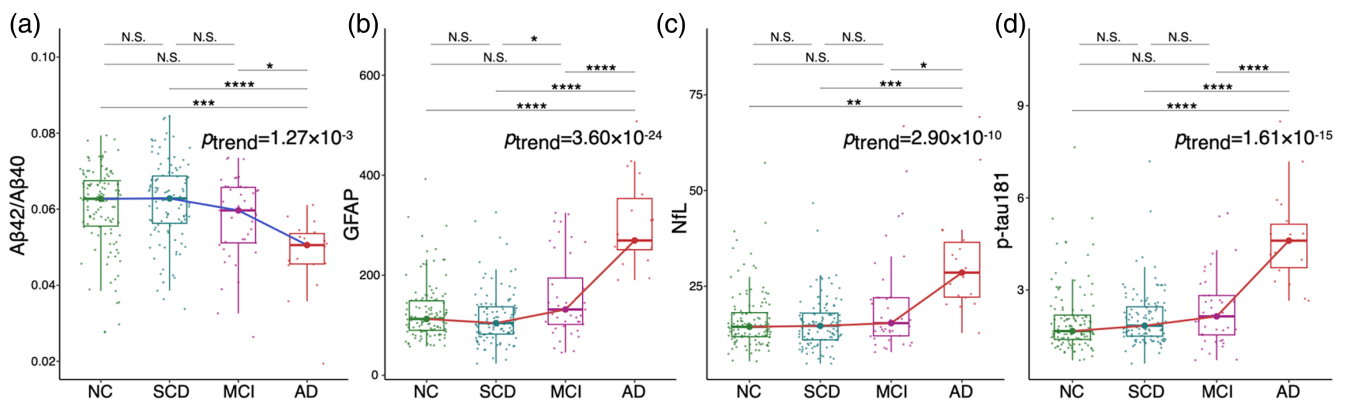
FIGURE 1 Distribution and significance of linear trends in plasma markers of Aβ42/Aβ40 (a), GFAP (b), NfL (c), and p-tau181 (d) among normal controls (NCs), subjective cognitive decline (SCD), mild cognitive impairment (MCI), and Alzheimer's disease (AD) groups. Aβ, β-amyloid; GFAP, glial fibrillary acidic protein; NfL, neurofilament light chain; p-tau181, phosphorylated tau181.

4.3 | Decreased network local efficiency with AD progression

Across the four diagnostic groups, we found a significant decreasing trend in the generalized local efficiency of the brain structural network in the imaging data set (linear trend: $t = -2.25$, $p = .025$; quadratic trend: $t = -2.58$, $p = .011$). Further analysis at the regional level revealed that 16 brain regions exhibited significant linea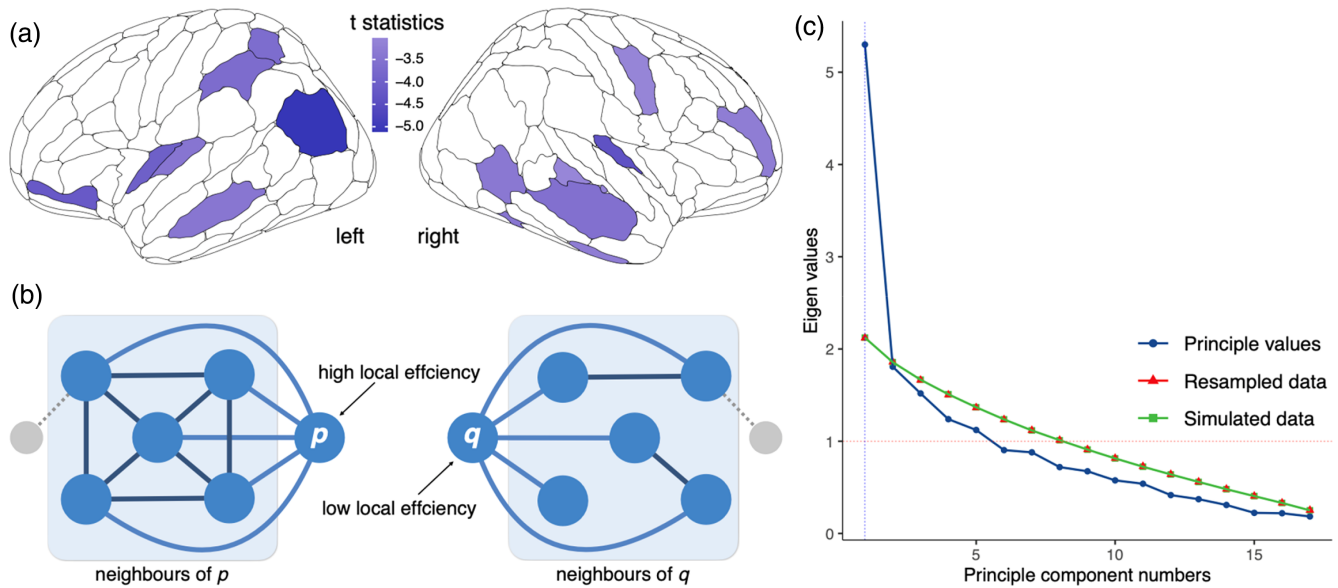r decreases ($p < .05$, corrected), mainly located in the bilateral frontal, temporal, parietal cortex, and subcortical regions (Figure 3a). Global efficiency and local efficiency did not show significant trends at either the whole-brain (Table S3) or regional level (Table S4).

We defined the 16 brain regions with a significant linear trend ($p < .05$, corrected) as AD progression-related regions (ADPRs). Then, we extracted the first principal component of generalized local efficiency across ADPRs with the *principal* function from the *psych* package (Figure 3c). The number of components was set to 1, as
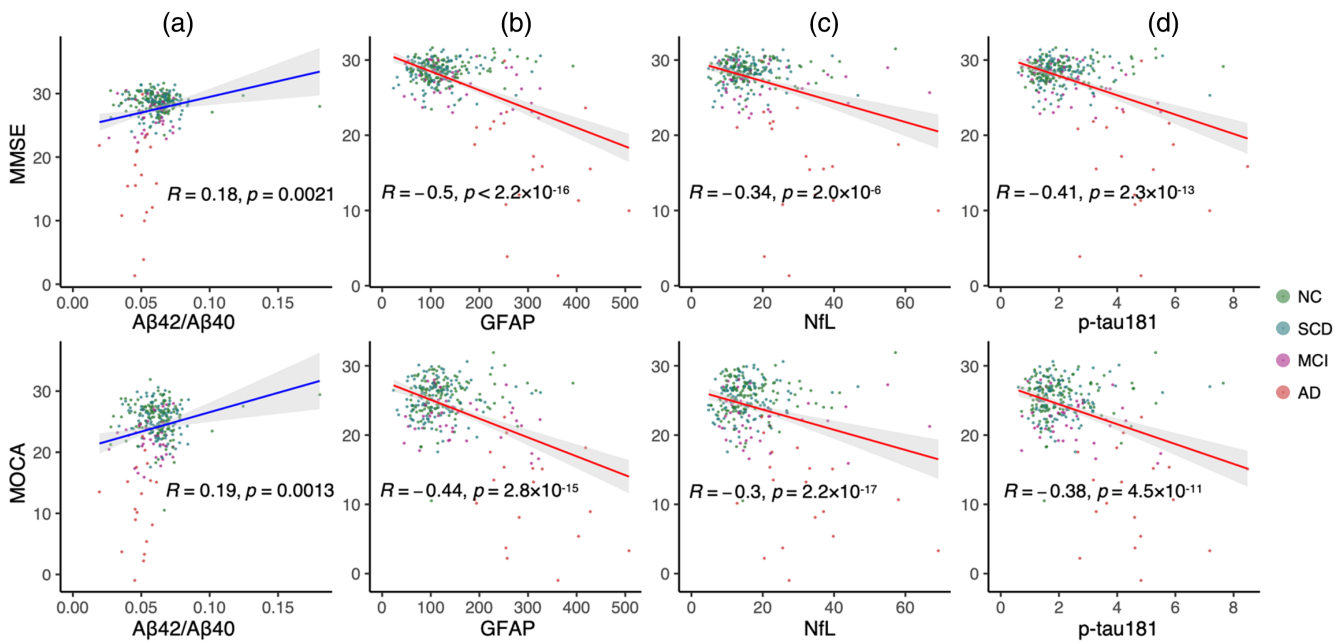
FIGURE 2 Correlations between plasma markers and general cognition. Correlations were controlled for age, sex, years of education, and APOE4 status (upper panel: MMSE; lower panel: MOCA). Aβ, β-amyloid; AD, Alzheimer's disease; GFAP, glial fibrillary acidic protein; MCI, mild cognitive impairment; MMSE, Mini-Mental State Examination; MOCA, Montreal Cognitive Assessment; NC, normal control; NfL, neurofilament light chain; p-tau181, phosphorylated tau181; SCD, subjective cognitive decline.


FIGURE 3 Local efficiency disruptions and principal component analysis. (a) Brain regions exhibited a significant linear decreasing trend of generalized local efficiency across the AD continuum ($p < .05$, FDR corrected). These regions were mainly located in the bilateral frontal, temporal, parietal cortex, and subcortical regions. (b) Higher local efficiency is associated with greater robustness to pathological changes. (c) Parallel analysis with 10,000 iterations suggested that the number of principal components was one. AD, Alzheimer's disease; FDR, false discovery rate.

suggested by a prior parallel analysis with 10,000 iterations. As higher local efficiency relates to greater robustness to pathological changes (Figure 3b), the small number of components suggested a highly covarying pattern among these regions, which may exhibit similar pathological changes across the AD continuum.

4.4 | Network disruption is related to cognitive decline and plasma markers

We further examined the correlation between network efficiency with plasma markers and cognitive performance in the combined data set.
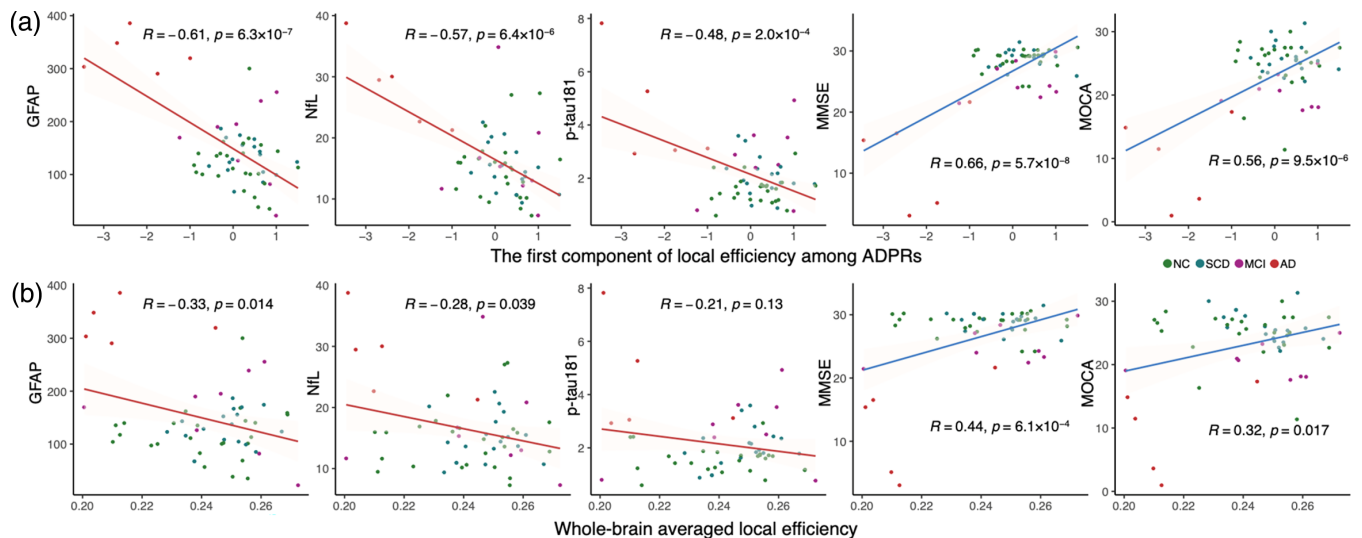
FIGURE 4 Relationship between local efficiency and plasma markers with cognition. The correlations of (a) the component of generalized local efficiency among AD-progression-related regions (ADPRs) were stronger than the correlations with (b) whole-brain averaged efficiency. These correlations were controlled for age, sex, years of education, and APOE4 status. Aβ, β-amyloid; AD, Alzheimer's disease; GFAP, glial fibrillary acidic protein; MMSE, Mini-Mental State Examination; MOCA, Montreal Cognitive Assessment; MCI, mild cognitive impairment; NC, normal control; NfL, neurofilament light chain; p-tau181, phosphorylated tau181; SCD, subjective cognitive decline.
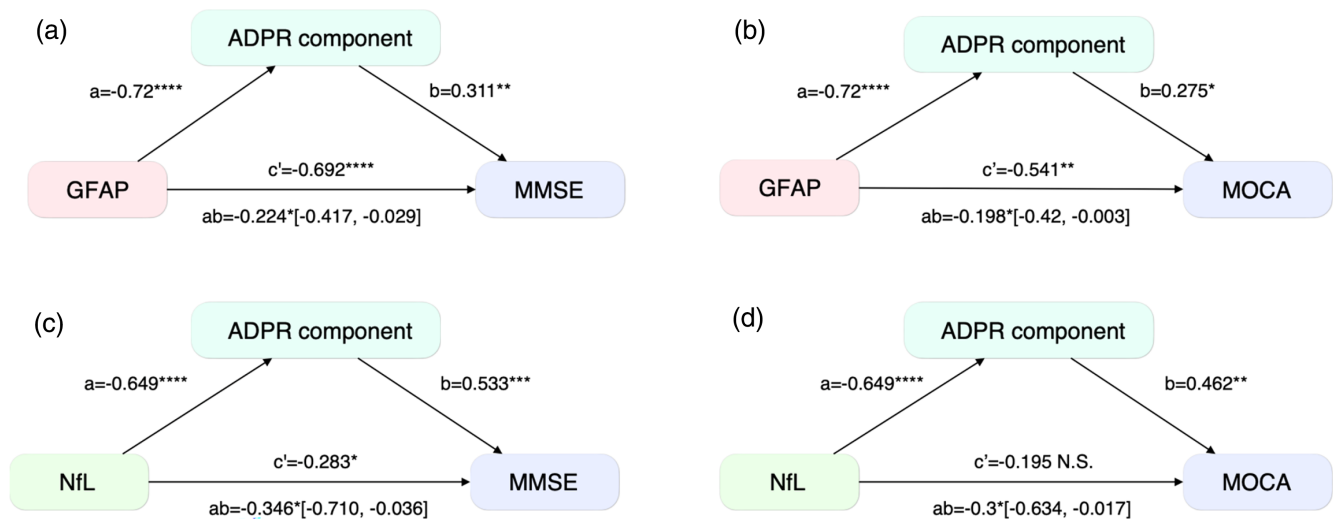
FIGURE 5 Local efficiency mediates the relationship between plasma markers and cognition. GFAP-MMSE (a), GFAP-MOCA (b), NfL-MMSE (c), and NfL-MOCA (d). This mediation effect was found in the AD-Progression-related Regions (ADPRs), determined through 10,000 bootstrapping. The 95% confidence intervals of the indirect mediation effects are presented. GFAP, glial fibrillary acidic protein; MMSE, Mini-Mental State Examination; MOCA, Montreal Cognitive Assessment; NfL, Neurofilament light chain.

The component score of generalized local efficiency among ADPRs demonstrated significant correlations with cognitive performance (Pearson's $R = 0.66$, $p = 5.7 \times 10^{-8}$ for MMSE; $R = 0.56$, $p = 9.5 \times 10^{-6}$ for MOCA) and plasma markers sensitive to AD progression, including GFAP (Pearson's $R = -0.61$, $p = 6.3 \times 10^{-7}$), NfL ($R = -0.57$, $p = 6.4 \times 10^{-6}$), and p-tau181 ($R = -0.48$, $p = 2.0 \times 10^{-4}$). However, no significant correlation was observed with Aβ42/Aβ40 ($R = -0.068$, $p = .62$). Notably, the component score of ADPRs exhibited a stronger correlation with pathological and clinical measures (Figure 4a) compared to the whole-brain averaged local efficiency (Figure 4b).

The discrepancy may suggest the potential of ADPRs in predicting AD-related changes in plasma markers and cognitive decline. See Figure S3 for all the correlations between network efficiency measures and plasma markers as well as cognitive performances.

4.5 | Mediation analysis

To investigate the mediating role of network efficiency in the relationship between plasma markers and cognitive performance,

we conducted mediation analyses using both the ADPR component and whole-brain average local efficiency. We found a significant average causal mediation effect, determined through 10,000 bootstrapping, in the relationship between GFAP (ab = −0.224, 95% CI = [−0.417 to −0.029], p = .0196 for MMSE; ab = −0.198, 95% CI = [−0.42 to −0.003], p = .0438 for MOCA) and NfL (ab = −0.346, 95% CI = [−0.710 to −0.036], p = .0188 for MMSE; ab = −0.300, 95% CI = [−0.634 to −0.017], p = .0266 for MOCA) with cognitive performance (Figure 5). The direct effect of NfL on cognitive performance (β = −.283, p = .021 for MMSE; β = −.195, p = .107 for MOCA) was weaker than the indirect effects mediated by the ADPR score. Notably, we did not observe significant mediation effects through whole-brain averaged local efficiency on the relationship between any plasma marker and cognition. The significant indirect effects of the ADPR component on the relationship between plasma markers and MMSE scores were robustly observed under a range of bootstrap resample numbers ranging from 500 to 20,000 (Figure S4).

5 | DISCUSSION

Our investigation identified plasma markers and network efficiency highly sensitive to AD progression and cognitive decline. Plasma GFAP emerged as the most sensitive AD progression indicator, as it was strongly correlated with cognitive status. Generalized local efficiency demonstrated a significant downward trend in multiple regions as AD advanced, whose component was inversely correlated with plasma GFAP, NfL, and ptau181 but positively correlated with cognitive level (MMSE and MoCA). Integration of plasma biomarkers and magnetic resonance imaging may offer a minimally invasive, cost-effective approach for AD diagnosis, supported by their impact on cognition through network efficiency mediation.

Four plasma biomarkers showed significant trends in AD progression, including Aβ42/Aβ40, NfL, pTau181, and GFAP. Notably, GFAP exhibited the highest sensitivity, displaying significant variations at the early stage and increasing levels as the disease advanced (Abdelhak et al., 2022; Kim et al., 2023). The literature consistently supports the diagnostic utility of plasma biomarkers in AD, individually or in combination with other markers (Baiardi et al., 2022; Chatterjee et al., 2023; Cullen et al., 2021; Janelidze et al., 2020; Kim et al., 2023). Elevated plasma GFAP levels were observed in cognitively intact individuals with Aβ positivity, particularly distinguishing Aβ+ from Aβ− individuals (Chatterjee et al., 2022). GFAP emerged as the earliest and most significantly altered biomarker from preclinical to symptomatic AD, predicting progression and cognitive decline (Guo et al., 2023; Shen et al., 2023). While GFAP levels can be influenced by other neuroinflammatory factors (Abdelhak et al., 2022), integrating multiple plasma biomarkers with structural efficiency can enhance the precision of staging patients along the AD continuum. Associations between plasma biomarkers and cognitive changes were evident, with GFAP exhibiting notable sensitivity. Previous studies have also demonstrated a strong correlation between plasma GFAP levels and cognition in AD patients (Chatterjee et al., 2021; Shir et al., 2022),

further validating its diagnostic value in assessing AD trajectory and predicting progression.

We observed a significant declining trend in whole-brain generalized local efficiency from the cognitively normal stage to the SCD, MCI, and AD stages. Recent studies have shown a discernible decline in local efficiency as AD advances and a noteworthy correlation between network efficiency and hallmark pathological features of AD, such as Aβ deposition and tau tangles (Jonkman et al., 2020; Kocagoncu et al., 2020; Prescott et al., 2014). In conjunction with the literature, our findings underscore the potential of local efficiency as a noninvasive biomarker to detect AD-related brain pathological changes.

We found regional disruptions in both hub regions (insular and superior parietal lobule) and peripheral regions (inferior parietal lobule, lateral temporal lobe, striatum, orbital gyrus, and middle frontal gyrus). The literature on topological disruptions along the AD continuum (Daianu et al., 2015; Lo et al., 2010; Rasero et al., 2017; Yan et al., 2018) supports the outcomes of our investigation, highlighting the potential of network efficiency as a cost-effective, effective, and noninvasive biomarker for AD imaging. Moreover, we note that the distribution of ADPRs overlaps with the pathological progression frequently observed in the frontal, cingulate, precuneus, striatum, parietal, and lateral temporal cortices (Chen et al., 2023; Villemagne et al., 2018). The cerebral regions identified in our study closely align with confirmed sites of AD pathology deposition, strongly indicating that pathological deposition may contribute to deviations in local efficiency, ultimately resulting in cognitive decline. Overall, we propose that local efficiency may capture a broad spectrum of brain damage across different AD stages.

The mechanisms underlying the impact of pathological molecules on cognitive decline along the AD continuum are complex. Building upon the possible mediating effect of neuroimaging biomarkers on the link between cognitive function and plasma biomarkers, several plasma biomarkers, such as pTau181 and NfL, have been found to potentially impact brain network efficiency by altering WM microstructure (Nabizadeh, Balabandian, et al., 2022; Nabizadeh, Pourhamzeh, et al., 2022). In our study, we delved deeper into the intricate connections between these biomarkers, particularly GFAP and NfL. The relationship between NFL and specific network efficiency metrics may not be intuitive. Structural network efficiency predicts resistance to cognitive decline in the elderly at risk for AD (Fischer et al., 2021). Education impacts functional network efficiency in Alzheimer's patients (Kim et al., 2021). Our findings demonstrate that network efficiency mediates the NfL-cognition association. Deep learning-based cognitive function quantification validates graph theory-based brain network features. Increased NfL levels indicate neurodegeneration, but cognitive decline requires specific network efficiency impairment (He et al., 2021). These findings enhance our understanding of Alzheimer's cognitive decline mechanism. Importantly, we found that the principal component of local efficiency among AD pathological regions exhibited robust correlations with plasma biomarkers and cognitive function, surpassing the overall brain local efficiency. Notably, these mediation effects were only significant

within the principal components among ADPRs, rather than the average efficiency of the entire brain. This observation aligns with previous studies revealing significant reductions in local efficiency within the AD population (Sami et al., 2018). Moreover, individuals carrying the apolipoprotein E ε4 allele displayed even greater reductions in local efficiency, underscoring its role as a reliable and distinctive indicator across the AD continuum (Korthauer et al., 2018). Overall, our study contributes novel insights into the complex mechanisms driving pathological cognitive decline in the AD process, elucidating the pivotal role of network efficiency.

Several limitations should be considered in interpreting the findings of this study. First, it is important to note that this preliminary investigation was conducted at a single center with a relatively modest sample size. Future studies should involve larger sample sizes from multiple centers to enhance the robustness and generalizability of our results. Second, it is worth mentioning that not all participants in the SILCODE cohort had complete blood and imaging data, leading to the division of the cohort into separate data sets for analysis. Collecting comprehensive clinical data during recruitment would facilitate more thorough follow-up investigations. Third, it is noteworthy that amyloid-PET data were unavailable for all individuals with AD and MCI included in our study. Consequently, the diagnostic process relied primarily on clinical data and imaging markers (Dartora et al., 2021; Sheng et al., 2020). Future research should incorporate ample gold-standard evidence, including amyloid-PET imaging, to strengthen diagnostic validity. Finally, the sample size of the AD group was relatively small due to the focus on the ultra-early stage of AD in the SILCODE cohort, which aimed to track the potential conversion of NC and SCD to later stages of AD. To mitigate the impact of the varying sample sizes, we adopted a comprehensive approach by employing disease continuum models, enabling more inclusive analyses that encompass the entire participant cohort. Taking these limitations into consideration in future studies will enhance the validity and clinical applicability of our findings in the field of neurology.

6 | CONCLUSION

In conclusion, our study highlights the significance of plasma GFAP levels as a valuable indicator for the early detection and prognosis of AD. We also emphasize the utility of generalized local efficiency in relevant brain regions as a sensitive marker for tracking disease progression. Furthermore, our findings demonstrate the significant mediation of network efficiency among AD-related regions in the relationship between plasma markers and general cognition. These results underscore the potential of integrating brain network connectivity efficiency and plasma biomarkers as a cost-effective strategy for screening and diagnosing AD. Combining these approaches holds promise in enhancing the accuracy and efficiency of AD diagnosis and prognosis, ultimately benefiting patients and advancing our understanding of the disease. Further research in larger cohorts is warranted to validate and expand upon these findings.

AUTHOR CONTRIBUTIONS

Mingkai Zhang and Haojie Chen: Investigation; data curation; writing—original draft; writing—review and editing. **Weijie Huang**: Investigation; writing—original draft. **Tengfei Guo**: Data curation; writing—review and editing. **Guolin Ma**: Writing—review and editing. **Ying Han and Ni Shu**: Investigation; data curation; writing—original draft; writing—review and editing; supervision.

CONFLICT OF INTEREST STATEMENT

The authors declare no conflicts of interest.

DATA AVAILABILITY STATEMENT

The data that support the findings of this study are available from the corresponding author upon reasonable request.

ORCID

Mingkai Zhang https://orcid.org/0009-0001-9846-123X
Haojie Chen https://orcid.org/0000-0002-4362-1056
Weijie Huang https://orcid.org/0000-0002-2481-1188
Ying Han https://orcid.org/0000-0003-0377-7424

REFERENCES

Abdelhak, A., Foschi, M., Abu-Rumeileh, S., Yue, J. K., D'Anna, L., Huss, A., Oeckl, P., Ludolph, A. C., Kuhle, J., Petzold, A., Manley, G. T., Green, A. J., Otto, M., & Tumani, H. (2022). Blood GFAP as an emerging biomarker in brain and spinal cord disorders. *Nature Reviews. Neurology*, 18, 158–172.

Albert, M. S., DeKosky, S. T., Dickson, D., Dubois, B., Feldman, H. H., Fox, N. C., Gamst, A., Holtzman, D. M., Jagust, W. J., Petersen, R. C., Snyder, P. J., Carrillo, M. C., Thies, B., & Phelps, C. H. (2011). The diagnosis of mild cognitive impairment due to Alzheimer's disease: Recommendations from the National Institute on Aging-Alzheimer's Association workgroups on diagnostic guidelines for Alzheimer's disease. *Alzheimer's & Dementia*, 7, 270–279.

Andreasson, U., Blennow, K., & Zetterberg, H. (2016). Update on ultrasensitive technologies to facilitate research on blood biomarkers for central nervous system disorders. *Alzheimer's & Dementia*, 3, 98–102.

Anon. (2021). Alzheimer's disease facts and figures. *Alzheimer's & Dementia*, 17, 327–406. https://doi.org/10.1002/alz.12328

Baiardi, S., Quadalti, C., Mammana, A., Dellavalle, S., Zenesini, C., Sambati, L., Pantieri, R., Polischi, B., Romano, L., Suffritti, M., Bentivenga, G. M., Randi, V., Stanzani-Maserati, M., Capellari, S., & Parchi, P. (2022). Diagnostic value of plasma p-tau181, NfL, and GFAP in a clinical setting cohort of prevalent neurodegenerative dementias. *Alzheimer's Research & Therapy*, 14, 153.

Ballard, C., Gauthier, S., Corbett, A., Brayne, C., Aarsland, D., & Jones, E. (2011). Alzheimer's disease. *Lancet*, 377, 1019–1031.

Bassett, D. S., & Sporns, O. (2017). Network neuroscience. *Nature Neuroscience*, 20, 353–364.

Bellaver, B., Povala, G., Ferreira, P. C. L., Ferrari-Souza, J. P., Leffa, D. T., Lussier, F. Z., Benedet, A. L., Ashton, N. J., Triana-Baltzer, G., Kolb, H. C., Tissot, C., Therriault, J., Servaes, S., Stevenson, J., Rahmouni, N., Lopez, O. L., Tudorascu, D. L., Villemagne, V. L., Ikonomovic, M. D., ... Pascoal, T. A. (2023). Astrocyte reactivity influences amyloid-β effects on tau pathology in preclinical Alzheimer's disease. *Nature Medicine*, 29, 1775–1781.

Benedet, A. L., Milà-Alomà, M., Vrillon, A., Ashton, N. J., Pascoal, T. A., Lussier, F., Karikari, T. K., Hourregue, C., Cognat, E., Dumurgier, J., Stevenson, J., Rahmouni, N., Pallen, V., Poltronetti, N. M., Salvadó, G., Shekari, M., Operto, G., Gispert, J. D., Minguillon, C., ... Translational Biomarkers in Aging and Dementia (TRIAD) study, Alzheimer's and Families (ALFA) study, and BioCogBank Paris Lariboisière cohort. (2021). Differences between plasma and cerebrospinal fluid glial fibrillary acidic protein levels across the Alzheimer disease continuum. *JAMA Neurology*, 78, 1471–1483.

Bondi, M. W., Edmonds, E. C., Jak, A. J., Clark, L. R., Delano-Wood, L., McDonald, C. R., Nation, D. A., Libon, D. J., Au, R., Galasko, D., Salmon, D. P., & Initiative for the ADN. (2014). Neuropsychological criteria for mild cognitive impairment improves diagnostic precision, biomarker associations, and progression rates. *Journal of Alzheimer's Disease*, 42, 275–289.

Chatterjee, P., Pedrini, S., Ashton, N. J., Tegg, M., Goozee, K., Singh, A. K., Karikari, T. K., Simrén, J., Vanmechelen, E., Armstrong, N. J., Hone, E., Asih, P. R., Taddei, K., Doré, V., Villemagne, V. L., Sohrabi, H. R., Zetterberg, H., Masters, C. L., Blennow, K., & Martins, R. N. (2022). Diagnostic and prognostic plasma biomarkers for preclinical Alzheimer's disease. *Alzheimer's & Dementia*, 18, 1141–1154.

Chatterjee, P., Pedrini, S., Doecke, J. D., Thota, R., Villemagne, V. L., Doré, V., Singh, A. K., Wang, P., Rainey-Smith, S., Fowler, C., Taddei, K., Sohrabi, H. R., Molloy, M. P., Ames, D., Maruff, P., Rowe, C. C., Masters, C. L., Martins, R. N., & AIBL Research Group. (2023). Plasma Aβ42/40 ratio, p-tau181, GFAP, and NfL across the Alzheimer's disease continuum: A cross-sectional and longitudinal study in the AIBL cohort. *Alzheimer's & Dementia*, 19, 1117–1134.

Chatterjee, P., Pedrini, S., Stoops, E., Goozee, K., Villemagne, V. L., Asih, P. R., Verberk, I. M. W., Dave, P., Taddei, K., Sohrabi, H. R., Zetterberg, H., Blennow, K., Teunissen, C. E., Vanderstichele, H. M., & Martins, R. N. (2021). Plasma glial fibrillary acidic protein is elevated in cognitively normal older adults at risk of Alzheimer's disease. *Translational Psychiatry*, 11, 27.

Chen, K.-L., Xu, Y., Chu, A.-Q., Ding, D., Liang, X.-N., Nasreddine, Z. S., Dong, Q., Hong, Z., Zhao, Q.-H., & Guo, Q.-H. (2016). Validation of the Chinese version of Montreal cognitive assessment basic for screening mild cognitive impairment. *Journal of the American Geriatrics Society*, 64, e285–e290.

Chen, Y., Wang, Y., Song, Z., Fan, Y., Gao, T., & Tang, X. (2023). Abnormal white matter changes in Alzheimer's disease based on diffusion tensor imaging: A systematic review. *Ageing Research Reviews*, 87, 101911.

Cook, P. A., Bai, Y., Nedjati-Gilani, S., Seunarine, K. K., Hall, M. G., Parker, G. J., & Alexander, D. C. (2005). *Camino: Open-source diffusion-MRI reconstruction and processing*.

Cullen, N. C., Leuzy, A., Janelidze, S., Palmqvist, S., Svenningsson, A. L., Stomrud, E., Dage, J. L., Mattsson-Carlgren, N., & Hansson, O. (2021). Plasma biomarkers of Alzheimer's disease improve prediction of cognitive decline in cognitively unimpaired elderly populations. *Nature Communications*, 12, 3555.

Daianu, M., Jahanshad, N., Nir, T. M., Jack, C. R., Weiner, M. W., Bernstein, M. A., & Thompson, P. M. (2015). Rich club analysis in the Alzheimer's disease connectome reveals a relatively undisturbed structural core network. *Human Brain Mapping*, 36, 3087–3103.

Dartora, C. M., Borelli, W. V., Koole, M., & Marques da Silva, A. M. (2021). Cognitive decline assessment: A review from medical imaging perspective. *Frontiers in Aging Neuroscience*, 13, 704661.

Fan, L., Li, H., Zhuo, J., Zhang, Y., Wang, J., Chen, L., Yang, Z., Chu, C., Xie, S., Laird, A. R., Fox, P. T., Eickhoff, S. B., Yu, C., & Jiang, T. (2016). The human Brainnetome atlas: A new brain atlas based on connectional architecture. *Cerebral Cortex*, 26, 3508–3526.

Fischer, F. U., Wolf, D., Tüscher, O., Fellgiebel, A., Alzheimer's Disease Neuroimaging Initiative (2021). Structural Network Efficiency Predicts Resilience to Cognitive Decline in Elderly at Risk for Alzheimer's Disease. *Frontiers in aging neuroscience*, 13, 637002. https://doi.org/10.3389/fnagi.2021.637002

Guo, Y., Shen, X.-N., Wang, H.-F., Chen, S.-D., Zhang, Y.-R., Chen, S.-F., Cui, M., Cheng, W., Dong, Q., Ma, T., & Yu, J.-T. (2023). The dynamics of plasma biomarkers across the Alzheimer's continuum. *Alzheimer's Research & Therapy*, 15, 31.

He, Y., Wu, J., Zhou, L., Chen, Y., Li, F., & Qian, H. (2021). Quantification of cognitive function in Alzheimer's disease based on deep learning. *Frontiers in Neuroscience*, 15, 651920.

Hebert, L. E., Weuve, J., Scherr, P. A., & Evans, D. A. (2013). Alzheimer disease in the United States (2010–2050) estimated using the 2010 census. *Neurology*, 80, 1778–1783.

Jack, C. R., Bennett, D. A., Blennow, K., Carrillo, M. C., Dunn, B., Haeberlein, S. B., Holtzman, D. M., Jagust, W., Jessen, F., Karlawish, J., Liu, E., Molinuevo, J. L., Montine, T., Phelps, C., Rankin, K. P., Rowe, C. C., Scheltens, P., Siemers, E., Snyder, H. M., & Sperling, R. (2018). NIA-AA research framework: Toward a biological definition of Alzheimer's disease. *Alzheimer's & Dementia*, 14, 535–562.

Janelidze, S., Mattsson, N., Palmqvist, S., Smith, R., Beach, T. G., Serrano, G. E., Chai, X., Proctor, N. K., Eichenlaub, U., Zetterberg, H., Blennow, K., Reiman, E. M., Stomrud, E., Dage, J. L., & Hansson, O. (2020). Plasma P-tau181 in Alzheimer's disease: Relationship to other biomarkers, differential diagnosis, neuropathology and longitudinal progression to Alzheimer's dementia. *Nature Medicine*, 26, 379–386.

Jenkinson, M., Beckmann, C. F., Behrens, T. E. J., Woolrich, M. W., & Smith, S. M. (2012). FSL. *NeuroImage*, 62, 782–790.

Jessen, F., Amariglio, R. E., Buckley, R. F., van der Flier, W. M., Han, Y., Molinuevo, J. L., Rabin, L., Rentz, D. M., Rodriguez-Gomez, O., Saykin, A. J., Sikkes, S. A. M., Smart, C. M., Wolfsgruber, S., & Wagner, M. (2020). The characterisation of subjective cognitive decline. *Lancet Neurology*, 19, 271–278.

Jonkman, L. E., Steenwijk, M. D., Boesen, N., Rozemuller, A. J. M., Barkhof, F., Geurts, J. J. G., Douw, L., & van de Berg, W. D. J. (2020). Relationship between β-amyloid and structural network topology in decedents without dementia. *Neurology*, 95, e532–e544.

Kim, K. Y., Shin, K. Y., & Chang, K.-A. (2023). GFAP as a potential biomarker for Alzheimer's disease: A systematic review and meta-analysis. *Cell*, 12, 1309.

Kim, Y., Kim, S.-W., Seo, S. W., Jang, H., Kim, K. W., Cho, S. H., Kim, S. E., Kim, S. J., Lee, J. S., Kim, S. T., Na, D. L., Seong, J.-K., & Kim, H. J. (2021). Effect of education on functional network edge efficiency in Alzheimer's disease. *Scientific Reports*, 11, 17255.

Kocagoncu, E., Quinn, A., Firouzian, A., Cooper, E., Greve, A., Gunn, R., Green, G., Woolrich, M. W., Henson, R. N., Lovestone, S., & Rowe, J. B. (2020). Tau pathology in early Alzheimer's disease is linked to selective disruptions in neurophysiological network dynamics. *Neurobiology of Aging*, 92, 141–152.

Korthauer, L. E., Zhan, L., Ajilore, O., Leow, A., & Driscoll, I. (2018). Disrupted topology of the resting state structural connectome in middle-aged APOE epsilon4 carriers. *NeuroImage*, 178, 295–305.

Li, X., Wang, X., Su, L., Hu, X., & Han, Y. (2019). Sino Longitudinal Study on Cognitive Decline (SILCODE): Protocol for a Chinese longitudinal observational study to develop risk prediction models of conversion to mild cognitive impairment in individuals with subjective cognitive decline. *BMJ Open*, 9, e028188.

Lo, C.-Y., Wang, P.-N., Chou, K.-H., Wang, J., He, Y., & Lin, C.-P. (2010). Diffusion tensor tractography reveals abnormal topological

organization in structural cortical networks in Alzheimer's disease. *The Journal of Neuroscience*, 30, 16876–16885.

Mattsson, N., Cullen, N. C., Andreasson, U., Zetterberg, H., & Blennow, K. (2019). Association between longitudinal plasma neurofilament light and neurodegeneration in patients with Alzheimer disease. *JAMA Neurology*, 76, 791–799.

Moscoso, A., Grothe, M. J., Ashton, N. J., Karikari, T. K., Lantero Rodríguez, J., Snellman, A., Suárez-Calvet, M., Blennow, K., Zetterberg, H., Schöll, M., & Alzheimer's Disease Neuroimaging Initiative. (2021). Longitudinal associations of blood phosphorylated Tau181 and neurofilament light chain with neurodegeneration in Alzheimer disease. *JAMA Neurology*, 78, 396–406.

Nabizadeh, F., Balabandian, M., Rostami, M. R., Kankam, S. B., Ranjbaran, F., Pourhamzeh, M., & Alzheimer's Disease Neuroimaging Initiative (ADNI). (2022). Plasma neurofilament light levels correlate with white matter damage prior to Alzheimer's disease: Results from ADNI. *Aging Clinical and Experimental Research*, 34, 2363–2372.

Nabizadeh, F., Pourhamzeh, M., Khani, S., Rezaei, A., Ranjbaran, F., Deravi, N., & ADNI. (2022). Plasma phosphorylated-tau181 levels reflect white matter microstructural changes across Alzheimer's disease progression. *Metabolic Brain Disease*, 37, 761–771.

Nakamura, A., Kaneko, N., Villemagne, V. L., Kato, T., Doecke, J., Doré, V., Fowler, C., Li, Q.-X., Martins, R., Rowe, C., Tomita, T., Matsuzaki, K., Ishii, K., Ishii, K., Arahata, Y., Iwamoto, S., Ito, K., Tanaka, K., Masters, C. L., & Yanagisawa, K. (2018). High performance plasma amyloid-β biomarkers for Alzheimer's disease. *Nature*, 554, 249–254.

Ovod, V., Ramsey, K. N., Mawuenyega, K. G., Bollinger, J. G., Hicks, T., Schneider, T., Sullivan, M., Paumier, K., Holtzman, D. M., Morris, J. C., Benzinger, T., Fagan, A. M., Patterson, B. W., & Bateman, R. J. (2017). Amyloid β concentrations and stable isotope labeling kinetics of human plasma specific to central nervous system amyloidosis. *Alzheimer's & Dementia*, 13, 841–849.

Prescott, J. W., Guidon, A., Doraiswamy, P. M., Roy Choudhury, K., Liu, C., Petrella, J. R., & Alzheimer's Disease Neuroimaging I. (2014). The Alzheimer structural connectome: Changes in cortical network topology with increased amyloid plaque burden. *Radiology*, 273, 175–184.

Rasero, J., Alonso-Montes, C., Diez, I., Olabarrieta-Landa, L., Remaki, L., Escudero, I., Mateos, B., Bonifazi, P., Fernandez, M., Arango-Lasprilla, J. C., Stramaglia, S., Cortes, J. M., & the Alzheimer's Disease Neuroimaging Initiative. (2017). Group-level progressive alterations in brain connectivity patterns revealed by diffusion-tensor brain networks across severity stages in Alzheimer's disease. *Frontiers in Aging Neuroscience*, 9, 215.

Rubinov, M., & Sporns, O. (2010). Complex network measures of brain connectivity: Uses and interpretations. *NeuroImage*, 52, 1059–1069.

Sami, S., Williams, N., Hughes, L. E., Cope, T. E., Rittman, T., Coyle-Gilchrist, I. T. S., Henson, R. N., & Rowe, J. B. (2018). Neurophysiological signatures of Alzheimer's disease and frontotemporal lobar degeneration: Pathology versus phenotype. *Brain: A Journal of Neurology*, 141, 2500–2510.

Shen, X.-N., Huang, S.-Y., Cui, M., Zhao, Q.-H., Guo, Y., Huang, Y.-Y., Zhang, W., Ma, Y.-H., Chen, S.-D., Zhang, Y.-R., Chen, S.-F., Chen, K.-L., Cheng, W., Zuo, C.-T., Tan, L., Ding, D., Dong, Q., Jeromin, A., Yen, T.-C., & Yu, J.-T. (2023). Plasma glial fibrillary acidic protein in the Alzheimer disease continuum: Relationship to other biomarkers, differential diagnosis, and prediction of clinical progression. *Clinical Chemistry*, 69, 411–421.

Sheng, C., Sun, Y., Wang, M., Wang, X., Liu, Y., Pang, D., Liu, J., Bi, X., Du, W., Zhao, M., Li, Y., Li, X., Jiang, J., & Han, Y. (2020). Combining visual rating scales for medial temporal lobe atrophy and posterior atrophy to identify amnestic mild cognitive impairment from cognitively normal older adults: Evidence based on two cohorts. *Journal of Alzheimer's Disease*, 77, 323–337.

Shir, D., Graff-Radford, J., Hofrenning, E. I., Lesnick, T. G., Przybelski, S. A., Lowe, V. J., Knopman, D. S., Petersen, R. C., Jack, C. R., Vemuri, P., Algeciras-Schimnich, A., Campbell, M. R., Stricker, N. H., & Mielke, M. M. (2022). Association of plasma glial fibrillary acidic protein (GFAP) with neuroimaging of Alzheimer's disease and vascular pathology. *Alzheimer's & Dementia*, 14, e12291.

Shu, N., Wang, X., Bi, Q., Zhao, T., & Han, Y. (2018). Disrupted topological efficiency of white matter structural connectome in individuals with subjective cognitive decline. *Radiology*, 286, 229–238.

Tournier, J. D., Smith, R., Raffelt, D., Tabbara, R., Dhollander, T., Pietsch, M., Christiaens, D., Jeurissen, B., Yeh, C. H., & Connelly, A. (2019). MRtrix3: A fast, flexible and open software framework for medical image processing and visualisation. *NeuroImage*, 202, 116137.

Villemagne, V. L., Doré, V., Burnham, S. C., Masters, C. L., & Rowe, C. C. (2018). Imaging tau and amyloid-β proteinopathies in Alzheimer disease and other conditions. *Nature Reviews. Neurology*, 14, 225–236.

Wang, X., Huang, W., Su, L., Xing, Y., Jessen, F., Sun, Y., Shu, N., & Han, Y. (2020). Neuroimaging advances regarding subjective cognitive decline in preclinical Alzheimer's disease. *Molecular Neurodegeneration*, 15, 55.

Wang, Y., Ghumare, E., Vandenberghe, R., & Dupont, P. (2017). Comparison of different generalizations of clustering coefficient and local efficiency for weighted undirected graphs. *Neural Computation*, 29, 313–331.

Yan, T., Wang, W., Yang, L., Chen, K., Chen, R., & Han, Y. (2018). Rich club disturbances of the human connectome from subjective cognitive decline to Alzheimer's disease. *Theranostics*, 8, 3237–3255.

Yu, M., Sporns, O., & Saykin, A. J. (2021). The human connectome in Alzheimer disease—Relationship to biomarkers and genetics. *Nature Reviews. Neurology*, 17, 545–563.

SUPPORTING INFORMATION

Additional supporting information can be found online in the Supporting Information section at the end of this article.